- *Technical Paper* -

VERIFICATION OF MASONRY PROPERTIES IN AEM ANALYSISFOR BRICK INFILLED REINFORCED CONCRETE FRAMES

Arifa I. ZERIN*1, Hamed SALEM*2, Akira HOSODA*3 and Khan M. AMANAT*4

ABSTRACT

The present study focuses on the verification of masonry constituent properties for analytical investigationofthe in-plane cyclic behavior of brick infilled RC framesin AEM. The material properties were establishedand validated for bricks and mortars under restraining influence within masonry prisms. Consequently, the verified constituent properties were exploited to analyzesingle-story single-bay half-scaled bare and brick infilled RC frame models under in-plane increasing reverse cyclic load which showed substantially good agreement with the corresponding test results.

Keywords:masonry prisms, brick infill wall, Applied Element Method (AEM)

1. INTRODUCTION

Multistoried masonry infilled reinforced concrete (MIRC) buildings with soft ground stories are a popular construction practice in Bangladesh. Generally, in all framed structures in Bangladesh, bricks made from burned clay are used in partition walls serving as infills to the frames. Lack of knowledge of local masonry properties discourages local structural engineers from considering infill walls as structural components. As a consequence, it has become a common practice to exclude the stiffness and strength contributions of infills in structural analysis of MIRC buildings even under seismic loads. According to Asteris, P. G. et al.[1], the presence of infills provides a local as well as global increase in strength and stiffness depending on their extent and their position in the frames, affecting the distribution and intensity of the inertia forces generated in seismic excitation. This may initiate stress concentrations in certain regions of structures, causing localized cracking or unexpected brittle failures detrimental to overall performance of MIRC frames. Hence, it is essential for professional structural engineers to understand the effect of local masonry infills on the seismic performance of MIRC buildings in Bangladesh.

In this context, the objective of the present research focuses on establishing the material properties of locally available masonry components, i.e. clay brick units and mortars in the Applied Element Method and validate the analytical models by the experimental results of in-plane cyclic response of brick infilled RC frames[2].

2. LITERATURE REVIEW

2.1 Compressive Behavior of Masonry

Masonry is characterized as an anisotropic and inhomogeneous material composed of two materials of somewhat different properties: stiffer bricks and relatively soft mortar distributed at regular intervals. According to several compression tests of masonry prisms[3], [4], in the case of stronger and stiffer bricks with relatively softer mortar composition, the mortar in the bed joint exhibits a tendency to expand laterally more than the bricks because of its lesser stiffness. Then, the mortar is confined laterally at the brick–mortar interface by the surrounding bricks and joints. Consequently, shear stresses at the brick-mortar interface result in an internal state of stress due to the existing bond. This creates tri-axial compression in the mortar and bilateral tension coupled with axial compression in the bricks (Fig.1). Under tri-axial compression, the maximum crushing stress and strain of mortar increases with the confining stresses[5].

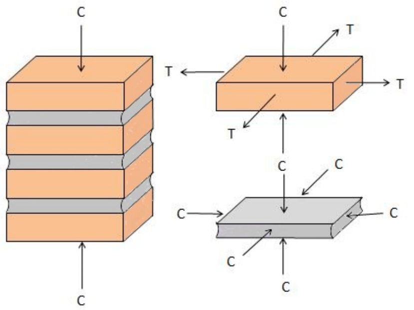

Fig.1 State of stresses in a masonry prism subjected to vertical compression[5]

*1 Graduate Student, Yokohama National University, Japan; Research Engineer, Housing and Building Research Institute, Bangladesh.
*2 Professor, Structural Engineering Department, Cairo University, Egypt.
*3 Associate Professor, Faculty of Urban Innovation, Yokohama National University, Japan.
*4 Professor, Department of Civil Engineering, Bangladesh University of Engineering and Technology, Bangladesh.

2.2 Failure Mechanism of Brick Prism

McNary and Abrams[3] conducted several uniaxial, biaxial, and tri-axial laboratory tests on clay bricks, mortars, and masonry prism considering nonlinear behavior of confined mortar between bricks and splitting strengths of bricks, revealing that mortar does not initiate failure of the prism due to the lateral confinement provided by the bricks. Consequently, the failure of masonry prisms initiates with lateral tensile splitting of bricks induced by the mortar.

2.3 Elastic Modulus of Bricks, Mortars and Masonry Prism

Micro and macro modeling of RC structures with brick infills requires inputting the material properties and constitutive relationships of masonry constituents. Since these material properties are not readily available due to the scarcity of laboratory tests and disparity in material properties geographically, Kaushik, Rai, & Jain[6] suggested simple relations for computation of the elastic modulus of bricks, E_b, mortar, E_j and masonry, E_m from their respective compressive strengths, f_b, f_j and f_m based on their experimental results and analyses, as follows:

$$E_b=300f_b \tag{1}$$
$$E_j=200f_j \tag{2}$$
$$E_m=550f_m \tag{3}$$

where all units are in MPa.

3. APPLIED ELEMENT METHOD

The Applied Element Method (AEM) proposed by Meguro and Tagel-Din[7] is based on the concept of discrete cracking where structural components are separated with elements connected through normal and shear springs. The stresses, strains, deformations, and failure of structures are successfully represented by each spring while Poisson's ratio of elements is neglected[7]. For concrete, AEM incorporates an elasto-plastic fracture model in compression[8] and linear stress-strain behavior in tension until cracks appear. The reinforcing steels are modeled considering the bare bar behavior for envelope[9] and Ristic model for hysteresis loops[10]. Moreover, generation of brick springs and brick-mortar interaction springs is included as in Fig.2[11] where K_b, and K_m are the stiffnesses of bricks and mortar respectively, whereas K_{eq} is the equivalent stiffness of brick-mortar interaction springs.

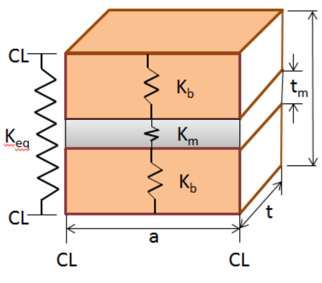

d =center to center distance of two consecutive brick units
a =length of brick unit
t = width of brick unit
t_m=thickness of mortar

Fig.2 Stiffness of brick spring and brick-mortar interaction spring in AEM[11]

According to Karbassi and Nollet[11], normal stiffness, K_n, and shear stiffness, K_s, of brick springs are calculated considering the element geometry illustrated in Fig.2 and incorporating elastic modulus of brick, E_b and shear modulus of brick, G_b, as follows:

$$K_n=E_b at/d$$
$$K_s=G_b at/d \tag{4}$$

Additionally, for brick-mortar interface springs, equivalent normal stiffness, K_{neq}, and equivalent shear stiffness, K_{seq}, are obtained considering element geometry (Fig.2), stiffness moduli of mortar (E_m and G_m) from the following equations:

$$1/K_{neq}=(d-t_m)/(E_b at)+t_m/(E_m at)$$
$$1/K_{seq}=(d-t_m)/(G_b at)+t_m/(G_m at) \tag{5}$$

Normal and shear springs of brick elements are affected in case of diagonal tension failure of masonry through brick units, whereas bond failure of masonry affects brick-mortar interaction springs[11]. It is also noted that shear-compression behavior is not currently included in the masonry wall model.

4. ANALYTICAL MODELS OF BRICK PRISMS UNDER UNIAXIAL COMPRESSION

4.1 Relevant Laboratory Test

A total of twelve masonry prism specimens were subjected to monotonically increasing uniaxial compression load to determine the ultimate compressive strength of masonry made of available constituent materials in Bangladesh[2].The commonly used size of brick units in Bangladesh is 240mm×115mm×70mm. For stretcher bond masonry prisms, five layers of half-scaled bricks with dimensions of 115mm×70mm×45mm and 1:4 mortars (Portland cement:local river sand) were used. The geometry of the masonry prisms was 230mm×230mm×70mm. The maximum compression loads and failure modes of the masonry prisms were investigated under two different loading conditions: six prisms out of twelve were subjected to a compression load perpendicular to the bed joints. The other six prisms were subjected toa compression load parallel to the bed joints.

4.2 Basic Assumptions in Models

For the masonry prism analytical model, the compressive strengths of bricks and mortars were determined considering the local constituent material properties in general. The elastic modulus of bricks and mortar was derived following Eq. 1 and Eq. 2[6]. Since Poisson's effect and tri-axial confining stress condition are not considered in the masonry wall constitutive model in AEM,the bond tensile strength atthe brick-mortar interface was assumed to be higher than the tensile splitting strength of bricks considering the failure initiated by splitting of bricks within prisms. Accordingly, extensive parametric studies were conducted to artificially generate confining stress condition in analytical models. The finally established constituent properties are illustrated in Table 1.

4.3 Verification of the Model

(1) Compression load perpendicular to bed joints

Under uniaxial compression load perpendicular to the bed joints, the test specimens exhibited three basic failure modes, i.e. crushing of mortar and bricks, shear compression failure of masonry and tensile splitting of bricks as in Fig.3(a), 3(b) and 3(c) respectively. The mean failure load was 131 kN. The test results varied due to inherent flaws existing in bricks, whereas, the analytical model failed at 177 kN load. Since, Poisson's effect is not included in the AEM model; it exhibited only crushing of bricks and mortar at interfaces (Fig.4b). Alternatively, global and principal stress and strain distribution (Fig.5) within the model clearly identified the tri-axial compression-tension-tension state of stress at the brick-mortar interface due to different elastic and shear moduliof the constituents, consequently generating the confining stress condition according to the assumption.

Table 1 Input constituent material properties

Properties	Brick	Mortar
Compressive Strength, MPa	17	11
Tensile Strength, MPa	1.6	1.9
Elastic Modulus, MPa	5170	2207
Shear Modulus, MPa	2414	883

(2) Compression load parallel to bed joint

The masonry prism test specimens exhibited tensile splitting of bricks along the shorter geometry direction as in Fig.6(a), 6(b) under average uniaxial compression load of 173 kN applied parallel to the bed joints. In addition, minor cracks along brick-mortar interfaces were observed as in Fig.6(c) due to uneven deformation characteristics of the constituent materials.The AEM model failed at 174 kN load with vertical tensile splitting of bricks (Fig.7b) due to tension induced by softer mortars of higher tensile strength compared to bricks, and showed substantially good agreement with the test results.

(a) (b) (c)

Fig.3 Failure mechanism of test specimens

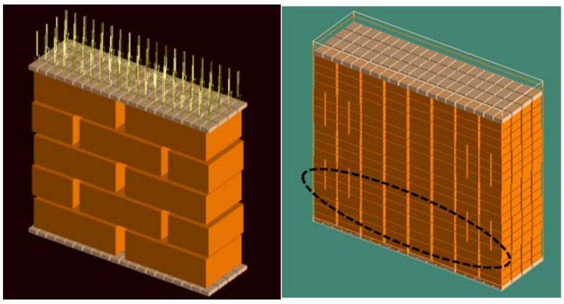

(a) (b)

Fig.4 (a) Analytical model: load perpendicular to bed joint, (b) Brick unit and mortar crushing

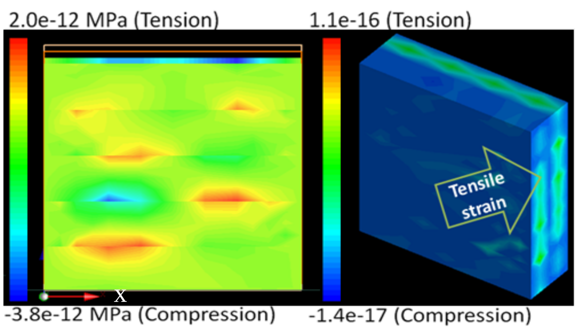

(a) (b)

Fig.5 (a) Global normal stress in x-direction, (b) Principal tensile strain in shorter direction

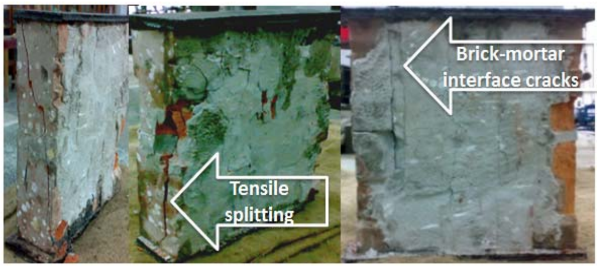

(a) (b) (c)

Fig.6 Failure mechanism of test specimens

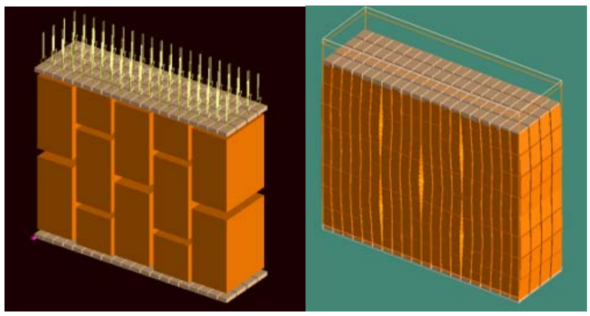

(a) (b)

Fig.7 (a) Analytical model: load parallel to bed joint, (b) Tensile splitting in brick units

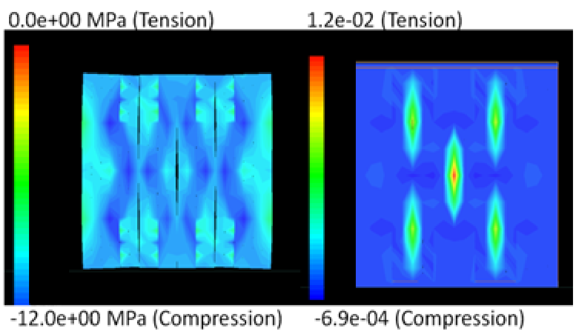

(a) (b)

Fig.8 (a) Minor principal stresses at failure, (b) Global strain distribution in transverse direction

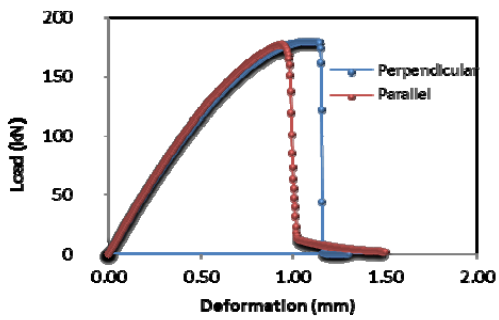

Fig.9 Load-deformation behavior of brick prism analytical models

Simultaneously, principal stresses and global strain distribution (Fig.8) within the masonry model clearly identified the stress trajectory after splitting of units. However, brick-mortar interface cracks and tensile splitting along the shorter direction did not occur in analysis as Poisson's effect is excluded in AEM.

(3) Maximum compressive strength of brick prism

The load-deformation behavior of brick prisms in the analytical models is illustrated in Fig.9, where a more accelerated strength drop is seen in the case of the compression load being applied perpendicular to the bed joint. Additionally, Table 2 compares the failure loads of the masonry prisms noted in the test specimens and AEM models. Average maximum compressive strength of brick prisms parallel to the bed joint was estimated from the test specimens and analytical model as 11 MPa (approx.). Moreover, average compressive strength perpendicular to the bed joint for AEM analysis was also calculated as 11 MPa (approx.), while the mean compressive strength estimated from the test results was about 8 MPa because of inherent inhomogeneity and flaws in the brick units.

5. ANALYTICAL MODEL FORBARE RC FRAME AND BRICK INFILLED RC FRAME UNDER IN-PLANE CYCLIC LOAD

5.1 Structural Models

Analytical models for a single-bay single-story bare RC frame and a locally available brick infilled RC framewere developed to evaluate their seismic performances and failure modes. Laboratory test results of bare RC frames and brick infilled RC frames under in-plane increasing reversed cyclic loads (Fig.10) obtained by Zerin and Amanat[2] were utilized to verify the analytical models. The dimensions along with the reinforcement details incorporated in both the test and analytical models are illustrated in Fig.11.For laboratory investigation of infilled frame, half-scaled local clay brick units (dimensions=115mm×70mm×45 mm) were used to construct aninfill wall 1525 mm high, 1525 mm wide and 100 mm thick.The analytical model was checked for mesh sensitivity and each brick unit was divided into 16 elements (4×4×1 elements) to ensure the possibility of crack propagation through bricks. The RC frame and the masonry infill were

Table 2 Failure loads of brick prisms[2]

Description	Direction of Load	Failure Loads (kN) M*	S_d**
Experiment	Perpendicular to Bed Joint	131	44
	Parallel to Bed Joint	173	42
AEM Analysis	Perpendicular to Bed Joint	177	
	Parallel to Bed Joint	174	

*M=Mean, **S_d= Standard Deviation

Fig.10 Brick infilled RC framespecimen under in-plane reverse increasing cyclic load[2]

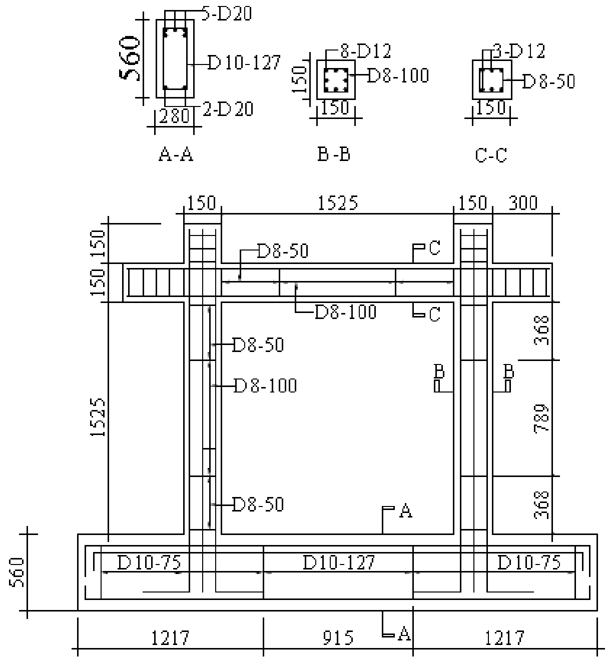

Fig.11 Geometry and reinforcement details of RC frame model[2]

Table 3 Average material properties in RC frame

Properties	Concrete	Steel
Compressive strength, MPa	32	-
Tensile strength, MPa	1.9	-
Elastic modulus, MPa	26897	200000
Shear modulus, MPa	11034	80000
Tensile yield strength, MPa	-	388
Ultimate strength, MPa	-	537

connected by mortar springs. The material properties of concrete and steel obtained from the laboratory tests are listed in Table 3.The input constituent material properties for the masonry prism models illustrated in Table 1 were utilized in the brick infilled RC frame

AEM model. In-plane increasing reverse cyclic loads (load controlled) were applied to the AEM models at the end elements of loading beam, which was the same as in test model (Fig.10).The boundary conditions of the AEM models were also kept same as test models by fixing the bottom elements of the base in the three directions and applying 178 kN compression loads on each fixing blocks modeled on the base.

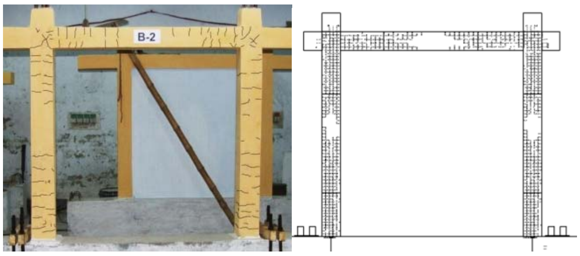

(a) (b)

Fig.12Crack patterns: (a) Test specimen (b) Analytical model

5.2 Verification of Analytical Model

(1) Bare RC frame

The crack patterns and load-displacement behavior of the AEM model for bare RC frames showed good agreement with the test results (Figs.12, 13). Flexural cracks initiated in columns both in the test specimens and analytical model at approximately 9 kN lateral load. As the load increased, tensile yielding of the steel embedded in the columns and beam was noted along with flexural cracks. X-cracks at beam-column joints due to inadequate shear reinforcement injoints also observed. The loading was stopped at 42 kN for test specimen to prevent total collapse. Whereas, the maximum shear capacity of the analytical model was about 50 kN.

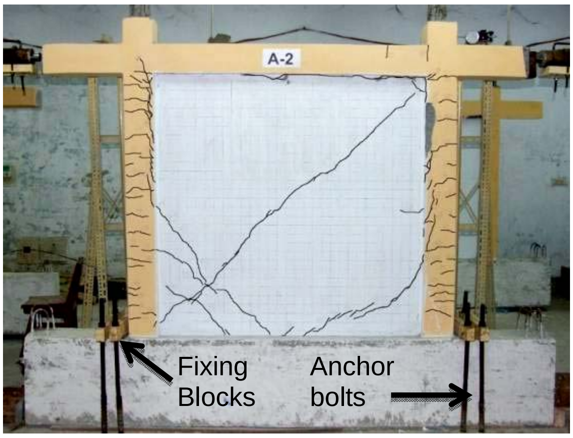

Fig.15 Crack propagation in test model at +178 kN lateral load

(2) Brick infilled RC frame

Hysteretic behavior, failure load, initiation and propagation of cracks through RC frames and infill in the analytical model showed substantially good agreement with the test results (Figs.14, 15, 16).Both the experimental and analytical models exhibited the same maximum shear capacity of 178 kN, which established the contribution of brick infills in enhancing the lateral stiffness of the frame by about 250% compared to bare RC frames. Under reverse cyclic increasing lateral load, the first cracks initiated in columnsdue to flexure at 89 kN load in the analyticalas well as in thetest models. Brick infills experienced first cracks nearly at 133 kN horizontal load in both cases. Later, either of the models failed principally due to

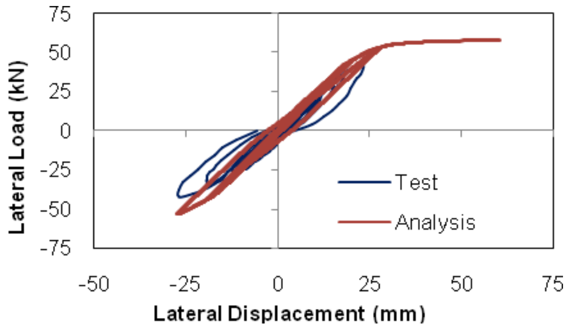

Fig.13 Hysteresis behavior of bare RC frames

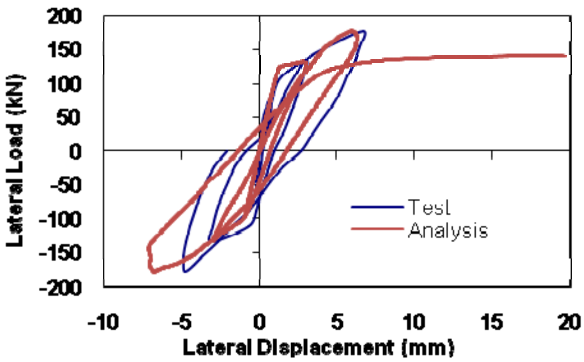

Fig.14 Hysteresis behavior of infilled RC frames

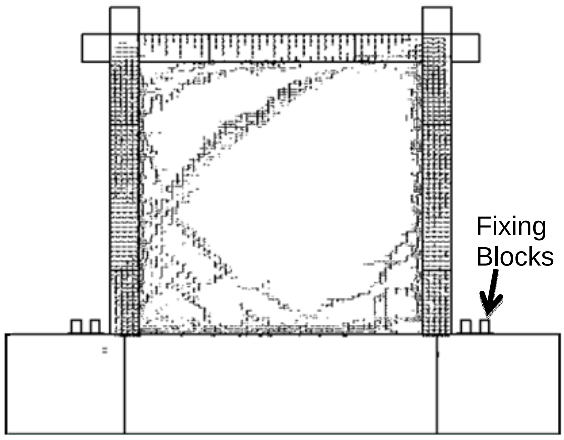

Fig.16 Crack propagation in AEM model at +178 kN lateral load

diagonal tension cracks in infills along with tensile yielding of longitudinal reinforcement in frames at 178 kN lateral load. Some shear cracks were also generated due to inadequate shear reinforcement in beam-column joints. However, diagonal tensile splitting of wall penetrating bricks proved the concept of higher bond tensile strength of mortar due to the confining effect of the surrounding masonry and RC frames both in the test and AEM models.

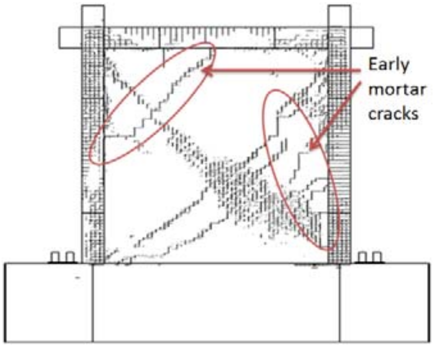

Fig.17 Effect of bond tensile strength ofmortar on crack propagation in infilled RC framed model

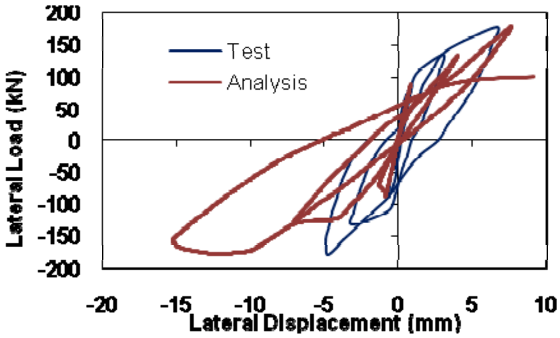

Fig.18 Effect of bond tensile strength of mortar on hysteresis behavior of infilled RC framed model

(3) Effect of bond tensile strength of mortar

The effect of the lower bond tensile strength of mortars was evaluated with an additional AEM model.The tensile strength of mortar was considered as 1.1 MPa (10% of mortar's compressive strength and 58% of its tensile strength in Table 1), while the other constituent properties were kept unchanged from those of the previous model, which are listed in Table 1 and Table 3. Relatively lower bond tensile strength of mortars in the AEM model initiated early tensile cracks in masonry propagated through bed and head joints (Fig.17) exhibiting sudden energy dissipation in hysteresis behavior (Fig.18) unlike in the test specimen which justifies the use of higher bond tensile strength of mortar in AEM brick infilled RC framed model.

6. CONCLUSIONS

The following conclusions are drawnfrom this research.

(1) The assumption of higher bond tensile strength atthe brick-mortar interface due to the confining effect of masonry has been successfully verified in both AEM models for masonry prisms and infilled RC frames.

(2) AEM simulation with the constituent material properties proposed by the authors showed good agreement with the experimental results of masonry prisms under uniaxial compression; in terms of failure load and crack patterns.

(3) The constituent material properties validated in masonry prisms were further successfully appliedin the brick infilled RC frame model in AEM where the analytical results exhibited substantially good agreement with the recorded strength and hysteretic deformation characteristics of the experimental results.

REFERENCES

[1] Asteris, P. G., Cotsovos, D. M., Chrysostomou, C. Z., Mohebkhah, A., and Al-Chaar, G. K., "Mathematical micromodeling of infilled frames: State of the art," Engineering Structures, vol. 56, pp. 1905–1921, 2013.

[2] Zerin, A. I. and Amanat, K. M. "Effectiveness of Ferrocement Laminates as a Repair and Retrofitting Material for Brick Infilled RC Frames," in JCI International Conference on Regeneration and Conservation of Concrete Structures, Jun 1st-3rd, Nagasaki, Japan, 2015 (submitted on 31 Dec, 2014).

[3] McNary, W. S. and Abrahams, D. P. "Mechanics of Masonry in Compression," J. Struct. Eng., vol. 111, no. 4, pp. 857-870, 1985.

[4] Atkinson, R. H. and Noland, J. L., "A Proposed Failure Theory for Brick Masonry in Compression," in 3rd Canadian Masonry Symp., vol. 5.1-5.17, Edmonton, Alta., Canada, 1983.

[5] Mosalam, K., Glascoe, L. and Bernier, J., "Mechanical Properties of Unreinforced Brick Masonry, Section 1," U.S. Department of Energy , Livermore, 2009.

[6] Kaushik, H. B., Rai, D. C. and Jain, S. K., "Stress-Strain Characteristics of Clay Brick Masonry under Uniaxial Compression," J. Materials in Civil Engineering, vol. 19, no. 9, pp. 728-739, September 2007.

[7] Meguro, K. and Tagel-Din, H. S. "Applied Element Method Used for Large Displacement Structural Analysis," J. Natural Disaster Science, vol. 24, pp. 25-34, 2002.

[8] Maekawa, K. and Okamura, H. "The deformational Behavior and Constitutive Equation of Concrete using the Elasto-plastic and Fracture Model," Journal of the Faculty of Engineering, The University of Tokyo (B), vol. 37, no. 2, pp. 253-328, 1983.

[9] Okamura, H. and Maekawa, K.,"Nonlinear Analysis and Constitutive Models of Reinforced Concrete," Tokyo: Gihodo, 1991.

[10] Ristic, D., Yamada, Y. and Iemura, H. "Stress-Strain Modeling of Hysteretic Structures under Earthquake Induced Bending and Varying Axial Loads," Kyoto, Japan, 1986.

[11] Karbassiand Nollet, M. J. "Performance-Based Seismic Vulnerability Evaluation of Masonry Buildings Using Applied Element Method in a Nonlinear Dynamic Based Analytical Procedure," Earthquake Spectra, vol. 29, no. 2, pp. 399-426, 2013.